TISSUE ENGINEERING: Part C
Volume 24, Number 6, 2018

DOI: 10.1089/ten.tec.2018.0062

termis
Tissue Engineering
& Regenerative Medicine
International Society

METHODS ARTICLE

Bioinspired Three-Dimensional Human Neuromuscular Junction Development in Suspended Hydrogel Arrays

Thomas Anthony Dixon, PhD,[1,2] Eliad Cohen, PhD,[3] Dana M. Cairns, PhD,[1] Maria Rodriguez, BS,[1] Juanita Mathews, PhD,[4] Rod R. Jose, PhD,[1] and David L. Kaplan, PhD[1,2]

The physical connection between motoneurons and skeletal muscle targets is responsible for the creation of neuromuscular junctions (NMJs), which allow electrical signals to be translated to mechanical work. NMJ pathology contributes to the spectrum of neuromuscular, motoneuron, and dystrophic disease. Improving *in vitro* tools that allow for recapitulation of the physiology of the neuromuscular connection will enable researchers to better understand the development and maturation of NMJs, and will help to decipher mechanisms leading to NMJ degeneration. In this work, we first describe robust differentiation of bungarotoxin-positive human myotubes, as well as a reproducible method for encapsulating and aligning human myoblasts in three-dimensional (3D) suspended culture using bioprinted silk fibroin cantilevers as cell culture supports. Further analysis with coculture of motoneuron-like cells demonstrates feasibility of fully human coculture using two-dimensional and 2.5-dimensional culture methods, with appropriate differentiation of both cell types. Using these coculture differentiation conditions with motoneuron-like cells added to monocultures of 3D suspended human myotubes, we then demonstrate synaptic colocalization in coculture as well as acetylcholine and glutamic acid stimulation of human myocytes. This method represents a unique platform to coculture suspended human myoblast-seeded 3D hydrogels with integrated motoneuron-like cells derived from human induced neural stem cells. The platform described is fully customizable using 3D freeform printing into standard laboratory tissue culture materials, and allows for human myoblast alignment in 3D with precise motoneuron integration into preformed myotubes. The coculture method will ideally be useful in observation and analysis of neurite outgrowth and myogenic differentiation in 3D with quantification of several parameters of muscle innervation and function.

Keywords: neuromuscular, 3D tissues, hydrogels

Introduction

PHYSIOLOGICALLY RELEVANT HUMAN three-dimensional (3D) tissues are increasingly being developed *in vitro* to explore human-specific tissue development and to elucidate specific pathophysiological processes. These engineered tissues often seek resemblance to the cytoarchitecture of tissues found *in vivo*, which may be difficult to obtain in two-dimensional (2D) culture with monolayers resting on artificial substrates.

While incredible progress has been made over the last century toward recreating developmental processes across various human tissue lineages, a consensus 3D model, for studying human neuromuscular junctions (NMJs) in skeletal muscle, remains to be achieved. These junctions are formed in the eighth to tenth week of development[1,2] as motoneurons extend out of the ventral root of the developing spinal cord and contact acetylcholine receptors in postjunctional folds on myotubes found in laterally expanding myotomes. These myotomes begin as a tissue layer in somites, bilateral blocks of mesoderm, which form parallel to the anterior–posterior axis of the embryo,[3] and eventually give rise to the muscular system.

This interaction between developing nerve and muscle is critically important in normal physiology and has pathological consequences in both congenital and acquired motoneuron diseases as well as in metabolic and dystrophic disorders of skeletal muscle.[4,5] Recreating this interaction

[1]Department of Biomedical Engineering, Tufts University, Medford, Massachusetts.
[2]Cell, Molecular, and Developmental Biology Program, Sackler School of Graduate Biomedical Sciences, Boston, Massachusetts.
[3]Department of Plastics Engineering, University of Massachusetts Lowell, Lowell, Massachusetts.
[4]Department of Biology, Tufts University, Medford, Massachusetts.

in vitro will improve options to study these diseases, and to test diverse pharmaceuticals, such as widely prescribed cholesterol-lowering statins, which are known to have a detrimental effect on skeletal muscle tissue, and in some cases may exacerbate peripheral neuropathy.[6,7]

Successful *in vitro* coculture of human myoblasts and stem cell-derived motoneurons in 2D was first demonstrated in 2011,[8] and more recently 2D human cocultures have developed further through using pluripotent cell lines and optogenetic stimulation of both cell types.[9–11] The transition to a 3D system remains important as cells grown on 2D tissue culture substrates are thought to differ considerably from cells grown in 3D environments in terms of cell morphology as well as in cell–cell and cell-matrix interactions; and overall 2D models are not thought to accurately mimic the native cellular microenvironment.[12–14] Existing 3D systems for developing aneural myotubes and coculturing neural cells with myoblasts have incorporated primary rat or murine cells and tissue or animal cell lines[15–20] rather than solely human stem cells or primary human cells.

Over recent years, human and animal aneural 3D muscle cultures have developed significantly, using diverse techniques, including hydrogel casting around flotation bars[21] and cantilevers,[22] stacking tissue sheets,[23] coculturing with endothelial cells,[24] and printing cell-laden extracellular inks.[25,26] To provide encapsulation of cells in 3D hydrogels, the hydrogel must be biocompatible, with suitable mechanical integrity and strength. As cantilevers can be removed from polydimethylsiloxane (PDMS) molds or fabricated silicon chips, this is a frequently pursued method, which has been demonstrated to form multiplexed arrays in past reports.[27–29]

While PDMS has continuously proven useful throughout tissue engineering, some critical limitations exist, including biological effects of leaching uncured oligomers, and absorption of bioactive hydrophobic molecules, including steroid hormones.[30] In addition, most techniques require casting, which may limit potential geometry, or micromachining, which can be cost prohibitive and not readily available to most cell biology laboratories.

Work in our laboratory has focused on finding an alternative biopolymer, which could be used to support 3D cell cultures and be printed *in situ* into tissue cultureware in arbitrary geometries. In related work, our laboratory recently reported on a cell-compatible freeform printing silk fibroin mechanism.[31] Silk fibroin is a natural biomaterial compatible with numerous polymers, notably extracellular matrix proteins, including collagens.[32] Silk fibroin solutions stored in high concentration 30% (w/v) will contain a high content of random coil and alpha helical structure, which will self-assemble into beta-sheet structures in a tunable timing ranging from hours to days and weeks, depending on the physiologic conditions used,[33] and solutions may be used as bioprinted polymer for mechanical support, or for cell encapsulation.[34,35]

Silk fibroin in sponge scaffolds have been previously shown in this context to support the differentiation of myotubes in 3D scaffolds, although the alignment is limited.[36] Alignment of myoblasts is a useful feature of 3D systems, including in this context, as a model composed of aligned human cells with functional contractility would allow more accurate drug and toxicity testing of human NMJs.[28] Improved *in vitro* testing is also useful in human disease models,[37] which are beyond the context of the present work. To the authors' knowledge, at the time of writing there remains no fully human innervated skeletal muscle model in 3D.

In this work, we seek to demonstrate 3D coculture through use of human cell types incorporating alignment features found in cast cell-seeded collagen around flexible posts[38] with the ability to create arbitrary geometries of natural polymer 3D culture supports using advances in freeform manufacturing, which may be implemented using technology and material widely available in tissue and biomedical engineering-focused laboratories.

We hypothesized that by providing primary human myoblasts a 3D environment, inspired by somite development, in combination with bioengineering a coculture of neural stem cell-derived motoneuron-like cells, we would support the formation of functional acetylcholine receptor expression on differentiated myotubes with synaptic colocalization similar to what is found in development. This outcome was anticipated in part on the prior demonstration in 3D coculture of differentiated or C2C12 myotubes and mouse embryonic stem cell-derived motoneurons[18] and past analyses of cell alignment in 3D hydrogels under tensile stress.[39] To test our hypothesis, a novel *in vitro* system to mimic aspects of the physical and biochemical environment responsible for NMJ formation *in vivo* was established.

Following our characterization of primary human myoblasts on 2D substrates, we demonstrate the growth and differentiation of myoblasts in an engineered 3D hydrogel, containing extracellular matrix. We then describe combined motoneuron-like cells in a coculture system designed to isolate individual aspects of gel compaction, tensile strength, and neurite isolation. We use this model to show that these cocultured tissue constructs can be assayed for excitability in a scalable, robust environment designed to make an array of constructs from one batch of cell-seeded hydrogels. The tissue coculture platforms described herein will be useful in studying the physiological nature of the interaction of motoneurons and differentiated myoblasts, and in using isolated disease-model cell types to recreate pathological phenotypes in a high-throughput setting.

Materials and Methods

Cantilever fabrication

Forty-percent silk fibroin solution (w/v) with 60-min extraction time was loaded into a 3-mL Nordson syringe and printed with a CellInk (Palo Alto, CA) Inkredible+ bioprinter through the pneumatic syringe holder. Nanoclay solution (2.5 g Laponite XLG in 50% w/v polyethylene glycol 400 in deionized H_2O was filled in the wells of 6-, 8-, 12-, or 24-well plates and the plates were loaded into the bioprinter plate holder. Code generated from slic3r and Repetier Host V1.6.1, with G-code modified with custom Python scripts, were sent to the bioprinter and the constructs were printed with pneumatic extrusion through 20–28G syringe tips at pressures of 15–80 kPa.

After the printing process was complete, prints were left in nanoclay solution for up to 12 h for silk polymerization (Supplementary Videos S1–S3; Supplementary Data are available online at www.liebertpub.com/tec). Prints were subsequently washed with phosphate-buffered saline (PBS) and left on a shaker plate overnight to remove nanoclay particles from silk. Before cell seeding, printed cantilevers were incubated at room temperature with 0.1% Pluronic

F127 to reduce gel adhesion to the culture surface and then ultraviolet (UV) sterilized for 20 min. Final cantilever dimensions in multi-well plates measure 5 mm high, 2 mm wide, and 6 mm across at the widest point. The two cantilevers are separated by distance of 6 mm and each cantilever sits atop a circular skirt with 1.5 mm radius.

Tissue engineering substrate

Silk fibroin solutions (hereafter referred to as silk) were purified following previously published procedures.[40] Briefly, silkworm cocoons were extracted in 0.02 M sodium carbonate to remove the sericin coating from the fibers. Fibers were then rinsed in distilled water, dissolved in 9.3 M lithium bromide (LiBr), and dialyzed against distilled water to remove LiBr. The resulting 7% w/v silk fibroin solutions were concentrated up to 15% w/v as needed and stored at 4°C until use. Other constituents of hydrogels include collagen type I and Matrigel (all materials from Sigma-Aldrich), used at a final concentration of 3 mg/mL of collagen I and 8% (v/v) Matrigel.

Cell culture

NG108-15 neuronal cells were obtained from American Type Culture Collection (ATCC, Manassas, VA). The cells were cultured in humidified 37°C/5% CO_2/95% air (v/v) environment in Dulbecco's modified Eagle medium (DMEM) containing 10% (v/v) fetal bovine serum (FBS), 1% (v/v) L-glutamine, 1% (v/v) penicillin/streptomycin, 2% sodium hypoxanthine, aminopterin, and thymidine supplement (materials from Thermo Fisher, Waltham, MA). Cells were seeded at 2.0×10^5 cells/cm^2 and FBS was removed from the media when optimal cell density ($\sim$70% confluence) was achieved to induce cell differentiation and neurite formation.

Primary human myoblasts were cultured in growth medium containing DMEM supplemented with 10% FBS, and 1% (v/v) penicillin/streptomycin (materials from Thermo Fisher). Cells were seeded at 5.0×10^5 cells/well of 12-well plates in 2D and 1×10^6 cells/mL of gelling solution in 3D. Confluence was kept below 80% during growth phase.

Human induced neural stem cells (hiNSCs)[41] were induced from reprogramming factors OCT4, KLF4, SOX2, and cMYC in a polycistronic lentivirus. hiNSCs were differentiated in DMEM/F12 with 1 μM purmorphamine, and 1 × B27/N2 for at least 12 days before coculture. Three-dimensional cocultures were initiated as differentiated motoneuron-like cells were concentrated through trypsinization and centrifugation, after which 5 μL of 1×10^7 cells/mL were directly pipetted on top of 3D freestanding myoblast-seeded construct. Liquid culture media was removed via aspiration before neural cell incorporation for more precise addition and to enable cells to adhere to the constructs without being mixed in culture solution. After 10 min to allow for neural attachment, a 1:1 ratio of myoblast and neural differentiation was applied as coculture media, and cocultures were cultured up to an additional 14 days.

Immunostaining

Cells and tissue constructs were fixed in 3.7% paraformaldehyde in PBS for 10 min. Following fixation, samples were washed in PBS and then permeabilized in 0.1% Triton X-100 and blocked in 1% bovine serum albumin for 1 h before staining. When staining with bungarotoxin, Alexa Fluor 647 conjugate constructs were stained prepermeabilization to visualize surface receptors. In all other cases, desmin (1:200), myoD (1:200), and alpha-actinin (1:200) (Thermo Fisher) were added after blocking solution and incubated overnight at 4°C.

Corresponding secondary antibodies with conjugated Alexa Fluor 555 and 488 dyes were added after three washes with PBS for five minutes each. Around 0.1% (vol/vol) 4′,6-diamidino-2-phenylindole (Sigma-Aldrich, all others from Thermo Fisher) was diluted in PBS and added to the samples in the absence of light at room temperature after removal of the secondary antibody, and washed three times with PBS. Samples were either mounted on microscope slides or left in PBS to avoid sample drying. Images were acquired on Keyence BZ-X700 or Leica SP8 Microscopes and analyzed with ImageJ and CellProfiler (Broad Institute, Cambridge, MA).

Strain deflection

Engineered tissue constructs were provided with static strain through attachment to printed and polymerized silk fibroin cantilevers. Strain models were simulated by analysis of deflection through measurement of the cantilever from neutral position. Force/displacement relationships were simulated for three tensile moduli found in literature for silk assembly mechanisms[42] similar to what is used in the present study. Cantilever was modeled in Autodesk Inventor with forces applied through half-loops of tensile muscle. Schematics were illustrated for visualization in Keyshot 3D rendering software.

Cellular orientation and scoring analysis

Cells were scored using basic pipelines freely available from CellProfiler.[43] Individual channels of fluorescent images in stacks were input into CellProfiler from ImageJ and were sorted into respective colors for cytoplasmic or nuclear staining based on filename. Sorted stacks were loaded in analysis modules used either for cell orientation identification or for scoring of positively labeled cells. Cell outlines, cytoplasmic staining, and nuclei are generated automatically by using Otsu's multiple thresholding algorithm[44,45] on the binned grayscale images (modules: IdentifyPrimaryObjects, IdentifySecondaryObjects, IdentifyTertiaryObjects) and identification, scoring, and morphological analysis were performed using downstream modules on individual pipelines (modules: MeasureObjectIntensity, measureObjectSizeShape, OverlayOutlines, RelateObjects, ClassifyObjects).

For cell orientation identification the modules MeasureObjectIntensity, measureObjectSizeShape, OverlayOutlines were used to generate morphological information on each profiled cell, where AreaShape_Orientation was used as a metric of cellular orientation ranging from 90° to –90°. Scoring of positive cells was performed by inputting cytoplasmic channels as child objects with nuclei channels as parent objects (RelateObjects) and classifying positive staining of nuclei through custom-defined bins with a ''0.5'' custom threshold corresponding to positive versus negative cytoplasmic staining surrounding identified nuclei [ClassifyObjects(RelateObjects)].

Data were output into ''.xlsx'' spreadsheets from CellProfiler, and subsequently transferred to GraphPad Prism 6 for generation and visualization of histograms, descriptive

statistics, and row mean with standard deviation (SD) or standard error of the mean (SEM).

Live imaging and analysis

Live cell imaging was performed on the Keyence imaging system with a heated stage and 5% CO_2 environment. While some constructs were able to be imaged *in situ*, in most analyses constructs were removed with micro tweezers and placed in an individual well with 1 mL Hank's Buffered Salt Solution (HBSS). Acetylcholine chloride or L-glutamic acid was added in a 10 or 150 mM bolus, respectively, of 10 μL to the well containing the construct with recording commenced ~5 s afterward, after readjustment of the microscopy stage and enclosure. For these experiments recordings took place over 120 s at 4–6 frames per second. Both mono- and cocultures were given the same acetylcholine bolus, and to detect the effect of diminished transmission from nerve to muscle, a final concentration of 8 μM tubocurarine was added to cocultured constructs.

To analyze calcium transients, recordings were saved as AVI files, and opened as an image stack in ImageJ. Z-projection of the image stacks with SD displayed heat maps of cells with calcium responses. For quantification, randomly chosen muscle fibers were traced as regions of interest (ROIs) and then measured for fluorescence over the 120 s study. Cellular fluorescence was normalized for the background, chosen as a dark area ROI, as well as baseline, which was established as an average of 5 s at the end of the recording. A representative recording for monoculture and coculture is shown, with three responding cells traced over the recording.

Confocal imaging

Confocal imaging was performed on an inverted Leica SP8 microscope equipped with white laser technology using a 10 or 20× water immersion objective with a numerical aperture of 1.0.

Real-time polymerase chain reaction

Gene expression levels for *MyoD*, myogenin (*MYOG*), Muscle-specific kinase (*MuSK*), human agrin (AGRN), myostatin (*MSTN*), and hypoxanthine-guanine phosphoribosyltransferase (*HGPRT*) were quantified by quantitative PCR. In brief, total RNA was extracted using the RNEasy Mini Kit (Qiagen, Valencia, CA), eluted, and quantified. The RNA extracted was reverse transcribed to cDNA in a 20 μL reaction using the iScript Advanced CDNA Synthesis Kit (Bio-Rad, Hercules, CA). Quantitative real-time polymerase chain reaction (RT-PCR) of cDNA (10 ng/μL) was performed using assays containing fluorescent hybridization probes (SYBR; Thermo Fisher).

Reactions were incubated at 95°C for 10 min and amplification was carried out on samples with 2 min incubation at 50°C, followed by 50 cycles of 15 s at 95°C and 1 min at 60°C. The reaction for RT-PCR was processed in a 10 μL solution containing 1 × Universal PCR Master Mix (Thermo Fisher) with 2 μL cDNA samples. RNA expression was compared with experimental controls using *HGPRT* as a reference gene. Results used with two trials of four technical replicates, with relative expression scored through the ΔΔCt method.

Primers had the following sequences: TGCCACAACGG ACGACTTC Human *MyoD1*-F 5′-CGGGTCCAGGTCTTC GAA-3′ Human *MyoD1*-R 5′-CACTCCCTCACCTCCAT CGT-3′, Human myogenin-F 5′-CATCTGGGAAGGCCAC AGA-3′, Human myogenin-R 5′-CTGGTTGCCTTCAGCG GAA-3′, *MUSK-F* 5′-CTGCACACATGAAAGTAGCCA-3′, *MUSK*-R 5′-GTCCTGCGTCTGCAAGAAGAG-3′, *AGRN*-F 5′-CTCGCATTCGTTGCTGTAGG-3′ *AGRN*-R 5′-ACCC CTGCCTAACCACATC-3′, *PAX7*-F 5′-GCGGCAAAGAA TCTTGGAGAC-3′, *PAX7*-R 5′-TCCTCAGTAAACTTCG TCTGGA-3′, *MSTN*-F 5′-CTGCTGTCATCCCTCTGGA-3′, *MSTN-R* 5′-CCTGGCGTCGTGATTAGTGAT-3′, *HPRT-1*-F 5′-AGACGTTCAGTCCTGTCCATAA-3′, *HPRT-1*-R.

Statistics

All statistical analyses in the text were performed with GraphPad Prism 6. As indicated throughout, paired or unpaired Student's *t* test was used where appropriate, and for the comparison of three or more groups, we used ordinary one-way analysis of variance followed by Dunnett's multiple comparisons test. Kolmogorov–Smirnov normality test was used where appropriate. N.s = not significant, $*p < 0.05$ level, Error bars are given as mean ± SEM.

Results

Cantilever modeling and sterile silk printing in tissue culture plates

Initial proof-of-concept experiments with culture of myoblast-laden hydrogels around cylindrical printed cantilevers were not successful as compacting gels did not have an anchor point and were found free floating in wells rather than forming a band around cantilever pairs. Cantilevers were then designed to have a T-shaped anchor, where compacting gels would form a loop around cantilever pairs. To ensure this design would be compatible with other myoblast-seeded hydrogel systems, which have produced forces up to 10 mN per construct,[46] an Autodesk Inventor simulation was run to evaluate if cantilevers would in theory displace in a linear relationship with force applied through muscle loops, and thus could be used as signal strength detection within limits of polymer failure.

The exact mechanism for silk dehydration and beta sheeting after nanoclay submerged bioprinting is a subject of active investigation, and the exact tensile strength would have to be confirmed through mechanical analysis, and may be batch specific and dependent on fine-tuned bioprinting conditions, making a generalized study out of the scope of this project. However, given similarities in terms of silk composition and drying techniques, the tensile modulus and strength are likely similar to prior studies of insoluble silk and in the range of 1–10 MPa.[42] Using these potential tensile moduli as a starting point of material properties in an Autodesk Inventor simulation of cantilever deflection, a linear relationship was shown between force applied on cantilevers and displacement of the cantilever beam face (Fig. 1A).

These T-shaped cantilevers were scaled to a 2 mm square base rising 3 mm to the cross beam, which is 6 mm across, 2 mm wide, and 2 mm tall. T cantilevers were set 6 mm apart and could fit in the center of a typical well in a 12-well plate. For manufacture, nanoclay solution was set into wells and a

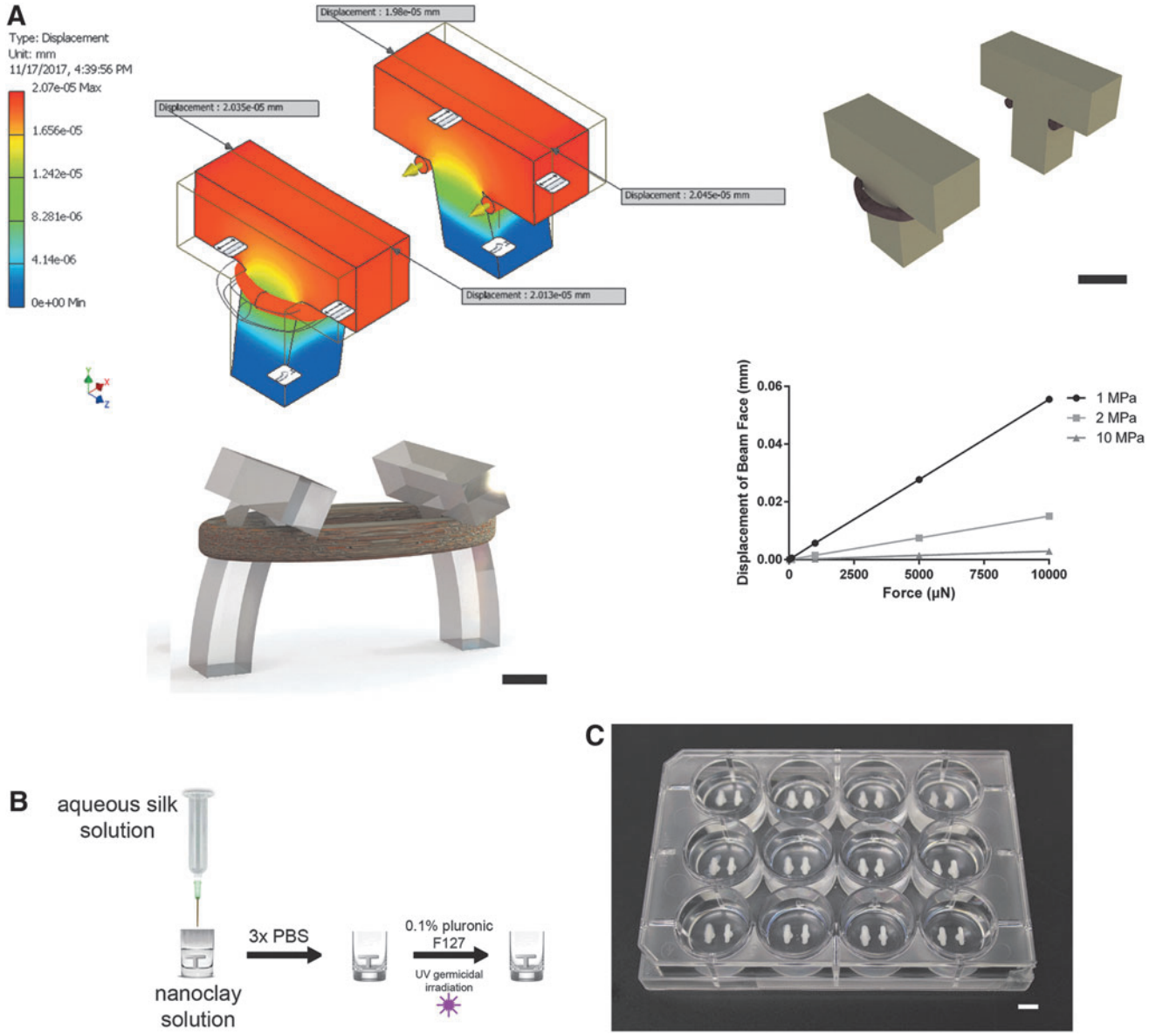

FIG. 1. Cantilever modeling and 3D freeform manufacture of silk cantilevers. **(A)** Autodesk Inventor capture of conceptual cantilever displacement for maintaining a suspended myoblast-laden gel with forces parallel to long axis of gel (*top left*). Autodesk Inventor static schematic showing silk cantilevers in beige, with muscle bundles in cross-section in *red* (*top right*). Keyshot 3D rendering of silk cantilevers displaced through compacting myoblast-laden hydrogel (*bottom left*). Cantilever displacement results at forces up to 10 mN at three different elastic moduli previously published in methods of silk beta-sheeting[42] from simulations in Autodesk Inventor (*bottom right*). **(B)** Schematic of 3D printing strategy for physically crosslinking aqueous silk into cantilever pair in tissue culture well with postprinting washing, and sterile preparation for cell seeding. **(C)** Photograph of a 12-well plate with replicated cantilever pairs for medium-throughput study. Scale bars: 2 mm **(A)**, 5 mm (*bottom right*). 3D, three-dimensional. Color images available online at www.liebertpub.com/tec

concentrated silk solution was extruded from 3-mL Nordson syringes using custom coding of Inkredible+ bioprinters (Supplementary Fig. S1).

Silk was incubated in nanoclay solution for 12 h at room temperature under sterile conditions in tissue culture hoods, after which nanoclay solution was washed out with successive PBS rinses, followed by UV germicidal irradiation (Fig. 1B). At this point, cantilever pairs in a 12-well plate (Fig. 1C) may be used with standard sterile tissue culture media, and for our purposes were incubated with myoblast-seeded hydrogels, generally with gels pipetted along the periphery of wells around the cantilever pairs so that they would compact into loops under the anchor of paired modeled and printed silk cantilevers.

Human skeletal myoblast differentiation with acetylcholine receptor clustering

Human primary skeletal myoblasts were purchased from Gibco® (Thermo Fisher) and expanded for 1–3 passages, where they contained significant fractions of muscle precursors positive for desmin and myoD when plated into 3D silk/

collagen/Matrigel gels (Supplementary Fig. S2), and exhibited a myogenic response to IGF-1 and recombinant human agrin (rhAgrin) treatment (Supplementary Figs. S2 and S3) after 14 days of differentiation. Collagen and Matrigel have long been used in combination as hydrogels for myotube engineering[47,48] and silk fibroin has been previously described for combinations in hydrogels and scaffolds with both collagen and Matrigel for support of several cell types, including adipocytes, neural cells, and osteocytes.[49]

We found a hydrogel composed of 3 mg/mL collagen I, 1% silk fibroin solution, and 8% Matrigel to be a suitable hydrogel in terms of myogenic differentiation in 2D (Supplementary Figs. S2 and S3) and in terms of mechanical integrity while compacting around silk cantilevers in 3D. While the 1% silk in hydrogel solution is at a low enough concentration to be unlikely to contribute substantially to hydrogel polymerization through beta sheeting after drying and incubation at 37°C, anecdotally, compacting hydrogel loops adhered better to printed silk cantilevers in 3D. This mechanism is incompletely understood, but may be related to the known properties of beta sheeting and self-assembly of silk fibroin proteins.[50]

To investigate the myogenic differentiation of human skeletal myoblasts (hSKMs) in plated silk/collagen/Matrigel, 3 mL of 1×10^6 hSKMs per mL hydrogel were seeded and polymerized through 1 h incubation at 37°C onto the surface of T75 flasks. After 3 days in growth medium and 4 weeks of subsequent incubation in differentiation medium after reaching 70–80% confluence, myoblasts were found differentiated isotropically with areas of local anisotropy. The hSKMs had proliferated on the plated gel culture and displayed alpha-actinin-positive multinucleated myotubes (Fig. 2). Upon staining with alpha-bungarotoxin, acetylcholine receptor clustering on mature myotubes was apparent along the length of several myotubes (Fig. 2). Acetylcholine receptor plaques provide a necessary maturity level for interaction of the distinct neuromuscular cell types *in vitro*.[51]

Anisotropic extension of myoblasts in engineered 3D suspended hydrogels

Engineered human skeletal muscle tissue constructs were encapsulated into silk/collagen/Matrigel hydrogels by combining 1×10^6 hSKMs in 3 mg/mL collagen I, 1% silk fibroin

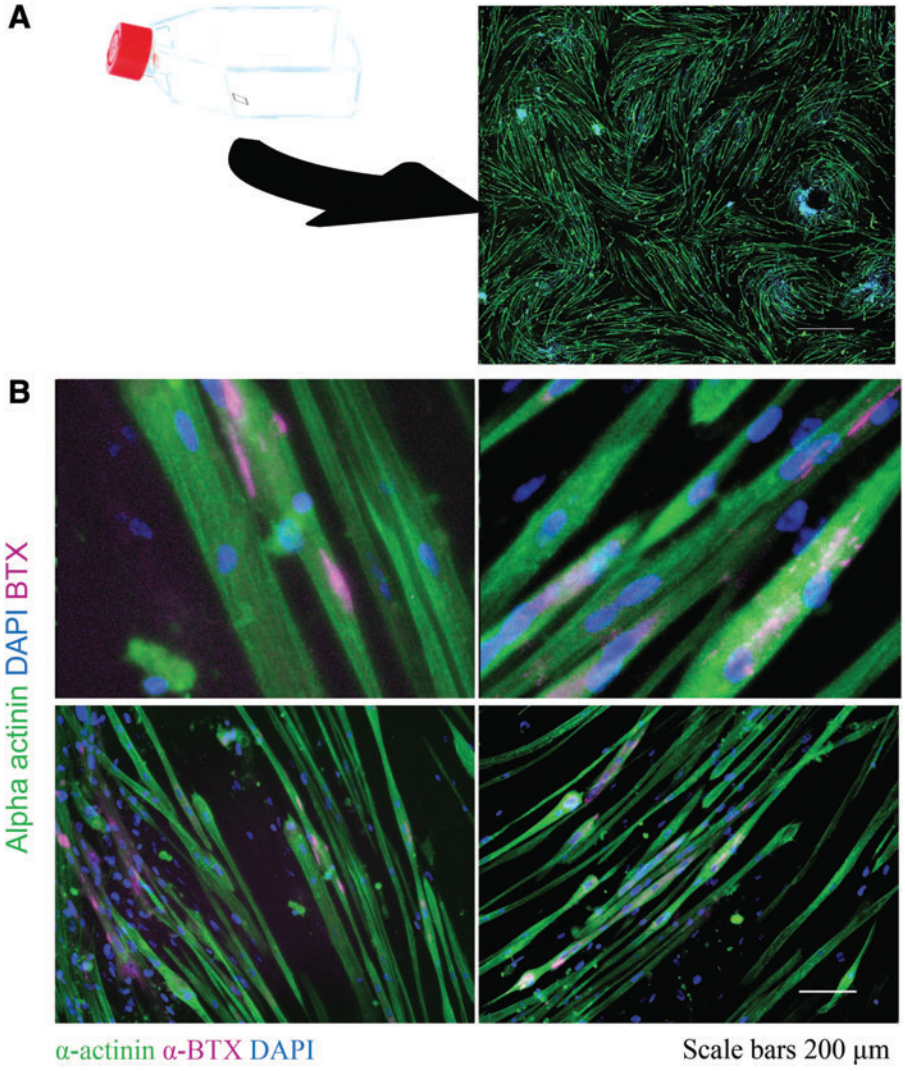

FIG. 2. Two-dimensional maturation of human myoblasts plated in silk/collagen I gel with potential for innervation. **(A)** hSKMs differentiated for 4 weeks displayed positive alpha-actinin (*green*) staining in multinucleated myotubes. Cells imaged in 6 mm × 6 mm area showed anisotropic alignment with localized areas of isotropic growth. **(B)** hSKMs differentiated for 4 weeks under the same conditions displayed punctate alpha-bungarotoxin staining (*pink*) in multinuclear myotubes with nuclei stained with DAPI (*blue*) shown in 10× and 40× (*bottom*) demonstrating elongated acetylcholine receptor formation. Scale bars 1 mm **(A)**, 200 μm [**(B)**, *top*] and 50 μm [**(B)**, *bottom*]. DAPI, 4′,6-diamidino-2-phenylindole; hSKM, human skeletal myoblast. Color images available online at www.liebertpub.com/tec

solution, and 8% Matrigel. After the cell-laden hydrogel is pipetted around the printed cantilever and polymerized at 37°C for 30 min, fresh growth medium is added and the gels lift off the plate. Control (''unattached'') 3D cultures consisted of pipetting of cell-seeded hydrogel around the periphery of tissue culture wells, with no printed substrate present. Three-dimensional hydrogels in controls would either partially lift off the plate or completely detach and be present in wells as a toroid of hydrogel (Fig. 3A).

When cell-seeded hydrogels were pipetted around the periphery of wells with printed T-shaped cantilever pairs present, the hydrogels compacted into a looped fascicular structure around the printed structure (Fig. 3B). Following three days of gel compaction and passive stress, low serum differentiation medium was applied, and the goal of confluence at 70–80% was estimated through brightfield visualization of cells elongating hydrogels in 3D. After 3 weeks in differentiation conditions, the *in vitro* tissue constructs with compacted hydrogels around printed T-shaped cantilever pairs contained densely aligned myofibers with a mean of at least 60% of cells having an orientation angle within 20° of the tension axis of the tissue through 21 days post-seeding, significantly higher than unattached controls without printed substrates at all time points (Figs. 3 and 4).

Differentiated myoblasts colocalize with extending neurites in 2D coculture

NG108-15 cells are a continuous neuronal cell line, which have been used in healthy and diseased NMJ models.[52,53] For initial tests of synaptic colocalization, NG108-15 cells and hSKMs grown in silk/collagen/Matrigel blends for 12 days of growth and 4 days of differentiation in co-culture media were shown to have desmin-positive myotube formation demonstrated by desmin-positive staining, as well as TuJ1-positive neurites extending out of the NG108-15 cell clusters and colocalizing with desmin-positive myoblasts (Supplementary Fig. S4). NG108-15 cells and C2C12 cells have been previously demonstrated as a cell line model for neuromuscular culture, however, to the

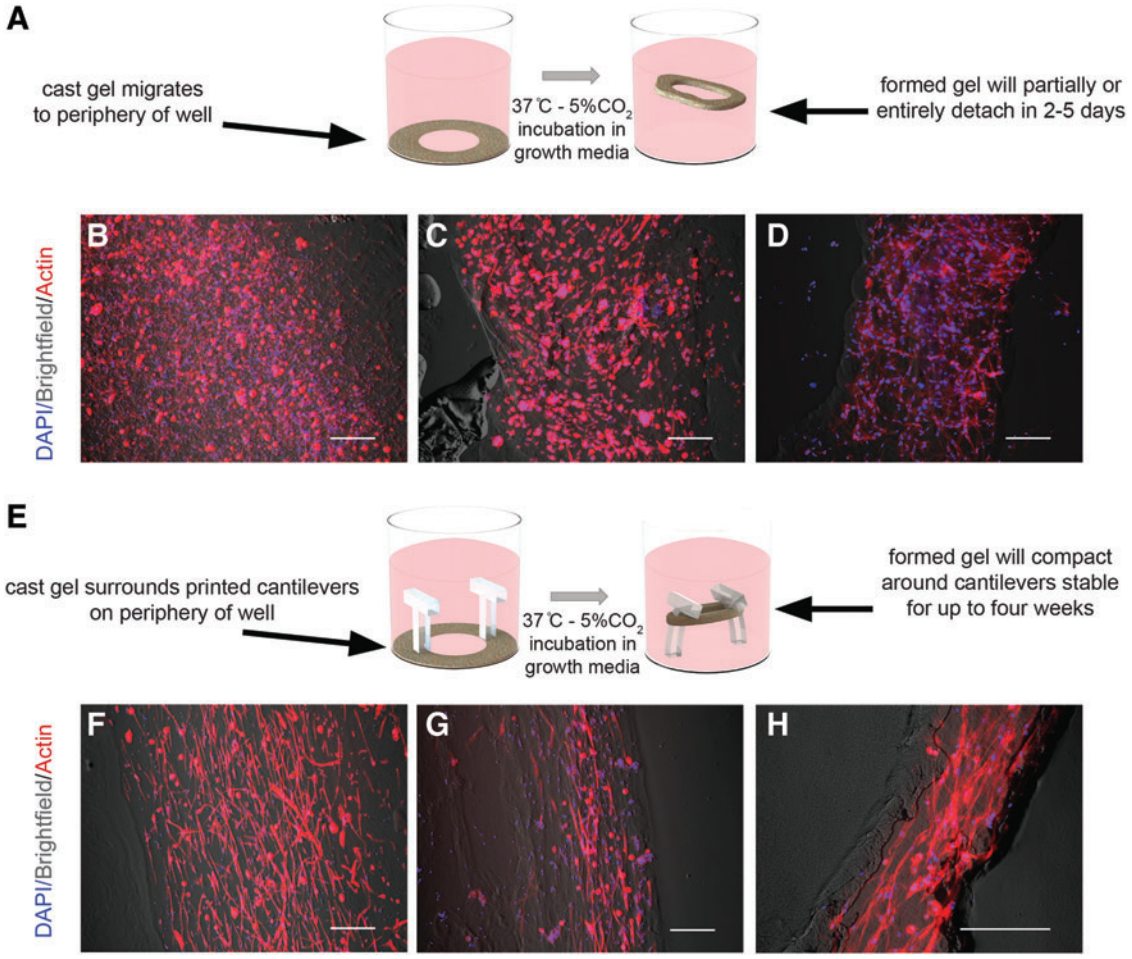

FIG. 3. Cell growth and anisotropic elongation in engineered silk/collagen/Matrigel hydrogels. **(A)** Representative IF of mounted myoblast-seeded gels differentiated at time points of 3, 7, and 21 days after seeding shown at 10× with phalloidin (actin) and DAPI staining. Hydrogel-seeded constructs in this series used standard 3D plated culture techniques with no substrate for gel compaction. **(B–D)** Representative IF of unmounted myoblast-seeded gels differentiated at time points of 3, 7, and 21 days after seeding shown at 10× with phalloidin (actin) and DAPI staining, with printed cantilever *insets* providing gel mounting **(E)** shown representatively **(F–H)**. Hydrogel-seeded constructs in the latter series compacted around 3D printed cantilevers. Scale bars: 200 μm. IF, immunofluorescence. Color images available online at www.liebertpub.com/tec

authors' knowledge, this is the first example of coculture with human myoblasts.

This coculture indicated viability of both cell types with the coculture media, and showed several instances of cells lining up along desmin-positive myoblasts, with interactions from cell clusters down the cytoskeletal level with a single myotube. While this coculture demonstrated the potential for viable coculture, a fully human model was desired for increased relevance to *in vitro* modeling. Toward this goal hiNSCs were differentiated with 1 μM purmorphamine for 12 days, adapted from a protocol to differentiate human induced pluripotent stem cells toward motoneurons.[10] After the differentiation protocol, a motoneuron-like phenotype positive for common motoneuron markers TuJ1, neural cell adhesion molecule (NCAM) and choline acetyltransferase was found (Supplementary Fig. S4), indicating a cholinergic neural phenotype.

Some evidence of early Schwann cell markers were seen in dense differentiating neurospheres through S100B, NCAM, and MBP staining (Supplementary Fig. S5). Human myoblasts cocultured in 2D with hiNSCs through plating of cell-seeded silk/collagen/Matrigel hydrogels showed evidence of maturation indicated by desmin staining, simultaneous with neurite extension through TuJ1 staining. Similar experiments were performed in 2.5-dimension (2.5D) coculture chips, where the motoneuron-like cells colocalized and spread on top of differentiated myotubes for 2 weeks, with TuJ1-positive hiNSCs extending neurites to desmin-positive myoblasts (Supplementary Fig. S4C).

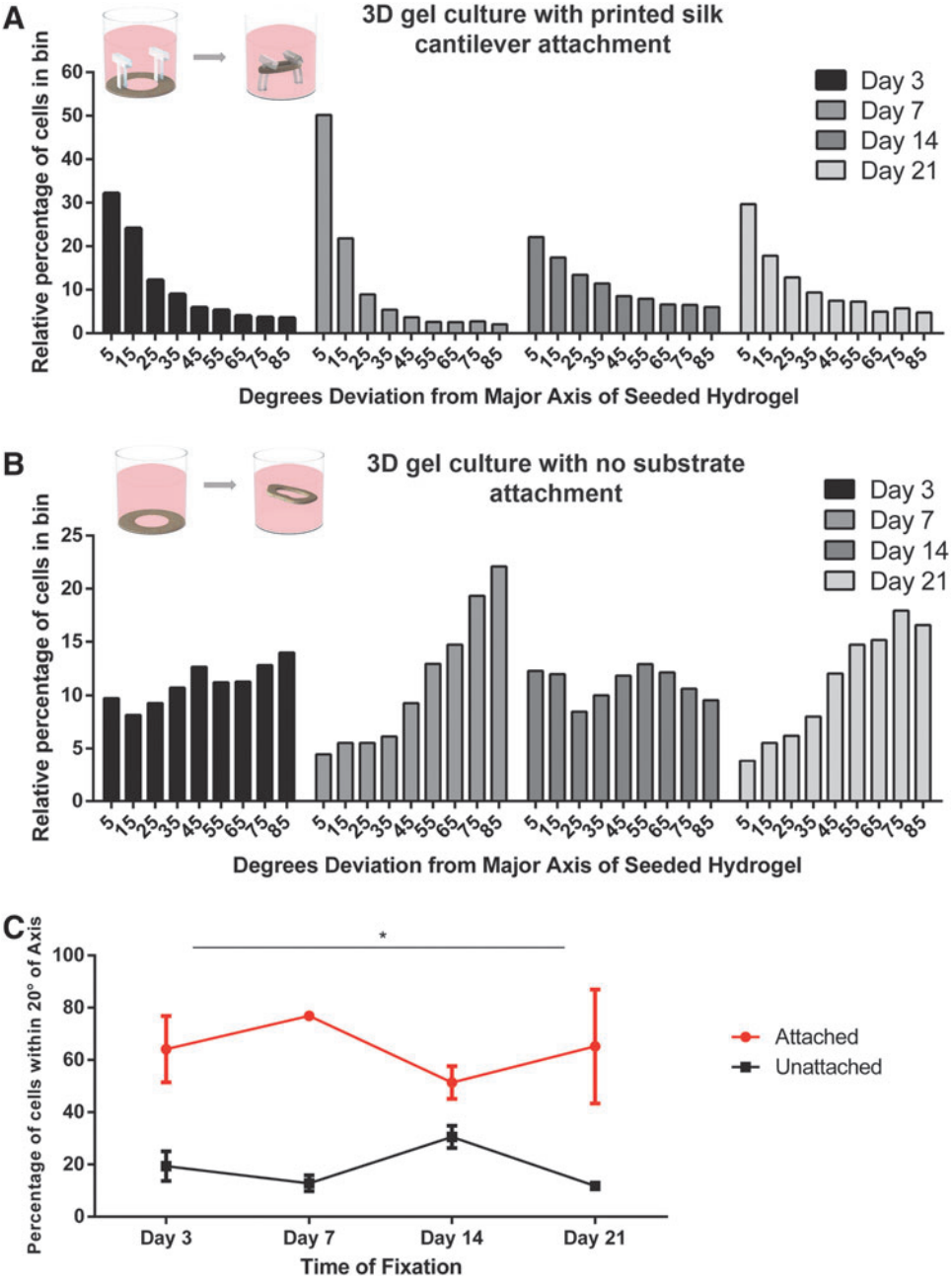

FIG. 4. Quantification of anisotropic elongation in engineered silk/collagen/Matrigel hydrogels. **(A)** Four individual histograms with relative cell orientation to long axis of printed substrate attached 3D hydrogels in 10° bins at four sacrificial time points. Each time point had $n = 3$ independent samples with the following combined binned cell count: 3048 cells (day 3), 1252 cells (day 7), 998 cells (day 14), and 522 cells (day 21). The *Y*-axis indicates the percentage of cells falling into bins with corresponding bin center ticked on *X*-axis. **(B)** Four individual histograms with relative cell orientation to long axis of 3D hydrogel without printed substrate ("unattached") in 10° bins at four sacrificial time points. Each time point had $n = 3$ independent samples with the following combined binned cell count: 3006 cells (day 3), 1304 cells (day 7), 649 cells (day 14), 1774 cells (day 21). As above, *Y*-axis indicates percentage of cells falling into bin with corresponding bin center ticked on *X*-axis. Samples were sacrificed in both groups from cell batch seeded in the same passage. **(C)** Row statistics of percentage of total binned cells falling within 20° of long gel axis with "attached" samples from **(A)** shown in *red*, with "unattached" samples from **(B)** shown in *black*. Statistical significance at all time points determined using the Holm–Sidak method, with alpha = 5.000%. Color images available online at www.liebertpub.com/tec

Cell alignment and hiNSC colocalization occurs in cell body segregated 2.5D chip culture and 3D freeform-printed suspended culture

After proof of concept of viable planar coculture, as a further intermediate step to 3D human neuromuscular coculture, we examined the alignment and differentiation of human skeletal muscle and differentiated human motoneuron-like cells in opposing channels of commercially available cell culture chips.[54] Microfluidic gel-embedded cell methods are sometimes referred to 3D culture, but often are referred to as 2.5D culture, where cells are seeded on or into a thin layer of Matrigel, other extracellular matrix,[55] or other fabricated multilayered thin channels.[56] In our system, human skeletal muscle myoblasts were seeded in silk/collagen/Matrigel hydrogel formulations described previously, and were found to align in 0.5 mm wide channels, throughout the length of the cell culture chip, $\sim$10.5 mm long.

These myoblasts showed anisotropic alignment throughout the channel as well as multinucleated myotubes indicating a degree of maturity similar to what is seen in the 3D suspended constructs (Supplementary Fig. S6). When hiNSCs were introduced into the opposing channel across from the seeded hydrogel, neurite extensions moved throughout the chip and colocalized along the multinucleated myotubes. The hiNSCs were also found to migrate along the length of myotubes (Supplementary Fig. S4C), indicating possible insoluble guidance cues on the myotube cell surface. While the focus of this method involves 3D human coculture, the ease of the 2.5D method using commercially available cell culture chips provides a screening method for using small amounts of reagents and cells while investigating coculture conditions before use of 3D models.

Formation of human 3D innervated functionally active muscle fibers

Heterogeneously cell-laden 3D suspended gels were investigated through the controlled addition of motoneuron-like cells to differentiated 3D myoblast cultures, typically beginning after 14 days of human myoblast monoculture. Three-dimensional myoblast monocultures were first differentiated for 14 days after seeding as described above with printed cantilever pairs present in culture wells. These myoblast seeded gels typically produced anisotropic alignment of myocytes as examined by antimyosin staining (MYH) (Fig. 5A). hiNSC-derived motoneuron-like cells were also visualized for cytoskeletal extension after 2 weeks of differentiation in 3D silk/collagen/Matrigel hydrogels, showing evidence of thin neurite extension (Fig. 5B).

To examine cytoskeletal colocalization of both cell types, 5 μL of 1×10^7 cells/mL of differentiated motoneuron-like cells were directly pipetted on top of 3D freestanding myoblast-seeded construct after 2 weeks of prior differentiation in monoculture. Cocultured constructs were then differentiated for 7–14 additional days in motoneuron differentiation media or in a 1:1 ratio of hiNSC and phenol-free myoblast differentiation media (Supplementary Fig. S7).

Visualized through confocal microscopy, alpha-bungarotoxin positive differentiated myoblasts were found to have extended throughout the seeded hydrogel with distinct localization from

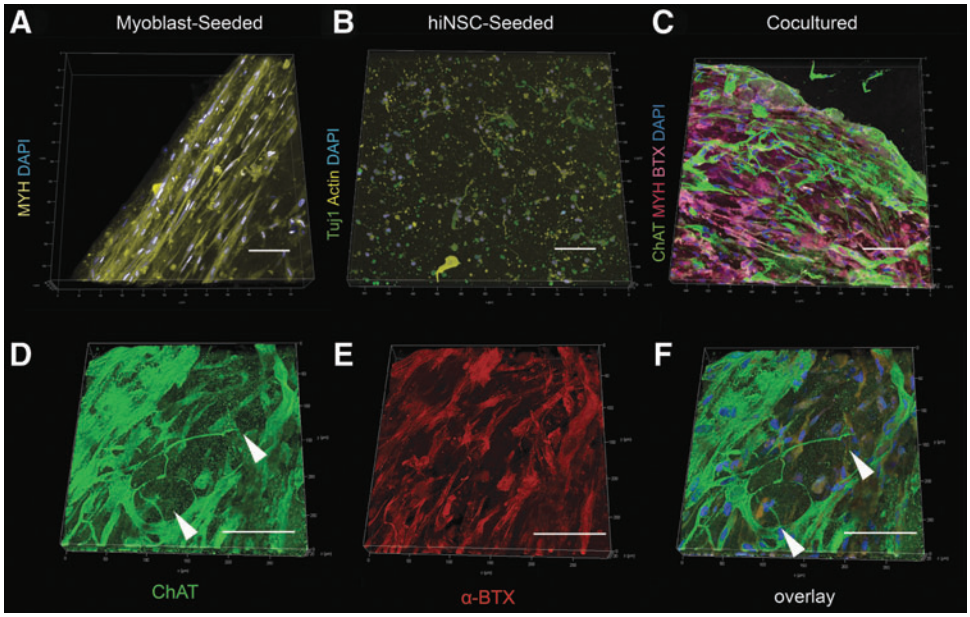

FIG. 5. Acetylcholine receptors aggregate in 3D monocultured myotubes and contact cholinergic neurite extensions in coculture with differentiated myoblasts and motoneuron-like cells. **(A)** Multichannel views of 3D monoculture culture gels grown for 14 days in suspended 3D culture with human skeletal muscle myoblasts differentiating anisotropically. **(B)** Monocultured hiNSCs extending neurites in monoculture after 2 weeks of differentiation. **(C)** Cocultured hiNSC neurites extending within myoblast-seeded gels after two additional weeks in coculture. DAPI nuclear stain, MYH, combined, alpha-bungarotoxin shown on *left*. **(D–F)** Differentiated alpha-bungarotoxin-positive myotubes contact hiNSCs propagating neurites colocalizing or extending along differentiated myoblast tracts. *X* and *Y* axes 600 μm long with 50 μm gridlines. Scale bars 100 μm (*left*). hiNSC, human induced neural stem cell. Color images available online at www.liebertpub.com/tec

motoneuron-like cells, which propagated regionally throughout the construct and stained positive for choline acetyltransferase (Fig. 5C). Specifically labeled motoneuron-like cells were appreciated through 10× magnification, and thin (<1 μm) neurites could be seen independently expressing specific cholinergic staining (Fig. 5D–F). This illustrates the potentiality for synaptic connection through colocalization of specific ChAT staining from neurites, with alpha-bungarotoxin-positive receptors found in myotubes.

To determine the functionality of monocultured and innervated 3D human myoblast-seeded hydrogels, we incubated constructs with Fluo-4 before detection of calcium fluxes. Live cell imaging was performed on the Keyence imaging system with a heated stage and 5% CO_2 environment. While some constructs could be imaged *in situ* on printed cantilevers, in most analyses constructs were removed with micro tweezers and placed in an individual well with 1 mL HBSS. Acetylcholine chloride was added in a 10 mM bolus of 10 μL to the well containing the construct and recording was commenced ~5 s afterward, after readjustment of the microscopy stage and enclosure, and recordings took place over 120 s at 4–6 image stacks with SD displayed heat maps of cells with calcium responses (Fig. 6A–E).

Randomly chosen cells were outlined as ROIs and then measured for fluorescence over the 120 s time course. Cellular fluorescence was normalized for the background, chosen as a dark area ROI, as well as baseline, which was established as an average of 5 s at the end of recording. Representative recordings for monoculture and coculture are shown, with three responding cells traced over the recording (Fig. 6B–E). Cells in both mono- and coculture had anisotropic calcium transients during the two-minute recordings (Supplementary Videos S4 and S5).

Cells were also stimulated with a final solution of 1.5 mM L-glutamic acid, where calcium transients were found, although transients were also found at baseline without stimulation, although to a lesser amplitude (Fig. 6F–I). Differentiated neurons were also exposed to cell tracers (CellTrace) before coculturing and exposed to L-glutamic acid. Putatively identified neurons (+CellTrace) and myocytes (–CellTrace/+Hoechst) were found to have differential response following glutamic blockade through tubocurarine, showing a lower level of depolarization (Fig. 6J–M) and thus glutamic acid-mediated activity of myotubes, putatively through neuromuscular connection.

Discussion

Tissue engineering methods, which explore the connection between motoneurons and myotubes, have developed substantially over the past decade, with an increasing complexity of techniques utilizing both 2D and 3D cultures. However, both 2D and 3D systems have drawbacks, including the use of nonhuman cell lines and a lack of anisotropy in engineering muscle tissue. To date, the authors have seen no report of an aligned human cell-derived 3D coculture system for studying the NMJ and neuromuscular functionality.

Notably, some 3D coculture systems with neuronal cells have been explored producing uniaxially oriented cells, allowing for measure of the gross contraction of the construct, but such models presently rely on rat or murine primary cells or cell lines.[18,57,58] Murine-derived cells are typically used in this context due to the additional expense and complexity involved in human primary cell culture, however, more widely commercially available primary human cells are becoming an attractive option to further translational relevance through human cell-derived tissue engineering strategies. To this end, numerous 2D coculture systems have been developed with distinct human cell types coplated in tissue culture plastic and coated glass, yet 2D systems generally suffer from a lack of recapitulation of the 3D architecture of normal tissue, and contain cells growing isotropically, in which myotubes are aligned parallel only in localized patchy regions.[11]

To combat these issues, strategies for the formation of 3D skeletal muscle suited to testing functionality are being actively sought in research. While much recent progress has been made in the field of engineering skeletal muscle in 2D and 3D, there is currently no consensus regarding the best method of 3D reproduction of human cocultures of human myoblasts and motoneurons. The method described in the present work provides a system, where motoneuron-like cells can be integrated into aligned 3D human myoblast-laden hydrogels, with healthy myotube formation and neurite extension through the gel. This method begins with a tunable system whereby cells can be seeded into hydrogels compacting around custom-designed 3D cantilever-supported freestanding 3D cultures, while maintaining use of standard tissue culture techniques and materials.

We first demonstrated a high degree of differentiation of myoblasts into myotubes in silk/collagen gels, in which the human myotubes produced distinct acetylcholine plaque formation after 4 weeks of differentiation. We then showed differentiation and reproducible anisotropic alignment of hSKMs in 3D hydrogels cast around sterile bioprinted silk cantilevers in tissue culture wells and differentiated for 3 weeks. In parallel experiments, hiNSCs were differentiated toward cholinergic motoneuron-like cell maturation, with widespread neurite extension. These cell types, along with NG108-15 cell lines, were successfully cocultured in 2D and 2.5D systems, with viability and specific phenotypic maturity shown for motoneurons and myotubes, including ChAT-positive hiNSC-derived motoneuron-like cells cocultured with desmin and alpha-bungarotoxin-positive hSKMs.

After successful 2D coculture, we demonstrated the feasibility of growing mature innervated human myotubes in our 3D system. Confocal z-stacking was used to investigate the nature of the mono- and cocultured constructs, and mature myotubes were present over several layers of the short axes of stacked cells (<50 μm) indicating differentiation in 3D.

Staining for alpha-bungarotoxin also showed colocalized AChRs along myotubes with ChAT-positive neurites in the construct thickness, illustrating the potential for synaptic connectivity of cholinergic neurons and acetylcholine receptors. Alpha-bungarotoxin was found to be diffusely expressed in human myotubes in 3D, similar to what has been found in prior reports,[59] which may indicate a less mature state of myotubes than what is found after similar time course of differentiation in 2D. Inducing the development of more mature plaque or ''pretzel'' formation[60] of acetylcholine receptors in 3D may have benefits in terms of synaptic connectivity, and is an active area of ongoing research.

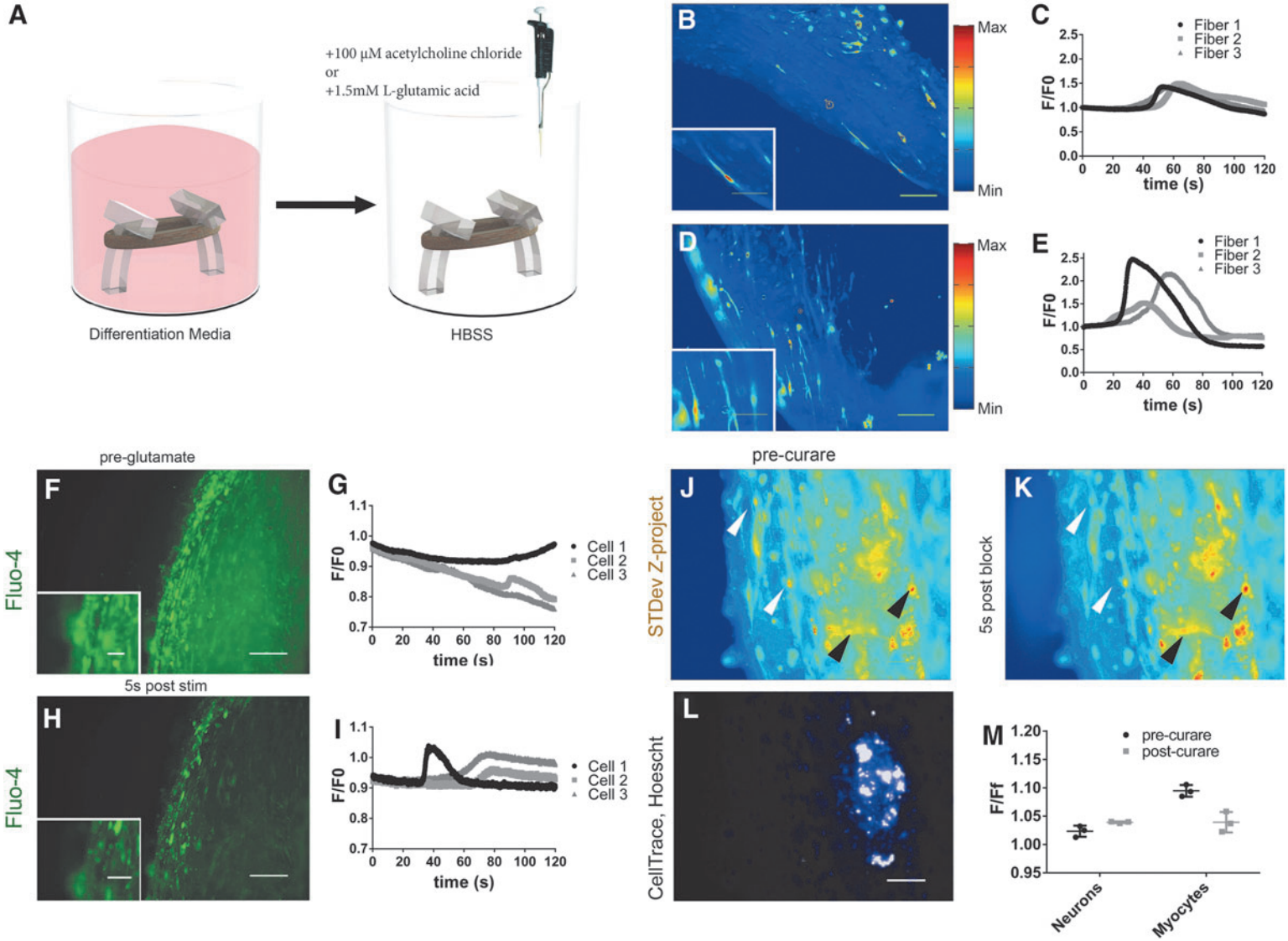

FIG. 6. Calcium flux responses to stimulation in mono- and cocultured 3D human cell-derived engineered constructs. **(A)** Three-dimensional monoculture myoblast-seeded gels grown for 28 days in suspended 3D culture, incubated for 1 h with Fluo-4 (Fluo-4 Calcium Imaging Kit; Thermo-Fisher) at 37°C. Individual wells on 12-well plates, containing constructs containing 1 mL of Hank's Buffered Salt Solution were given a 100 mM acetylcholine chloride bolus and recording was started 5 s following the bolus. **(B, D)** Standard deviation Z-projection of AVI file with five frames per second and total recording length of 120 s. Image is shown in "Jet" lookup table (LUT) (ImageJ) with *red* shift indicating movement, and *blue* shift showing low deviation (*left*). Graph of three cells outlined as ROIs (*yellow* outline, *left*) shown in traces on *right* **(C, E)**, with time 0 on chart indicating $t = 5$ s after acetylcholine bolus. Three traces are shown and are normalized to *dark* background (ROI # 4) as well as to baseline, taken as an average of 5 s at the end of recording. **(F–I)** Same as above with imaging of hiNSCs and hSKMs differentiated for 14 days before Fluo-4 incubation after L-glutamic acid stimulation. **(J–L)** hiNSCs incubated with CellTrace shown in coculture with glutamic acid stimulation before and after blockage with tubocurarine. **(M)** Relative fluorescence transient with identified neurons and myocytes before and after glutamate blocking agent. Scale bars 200 µm. ROI, regions of interest. Color images available online at www.liebertpub.com/tec

Through coculture in engineered 3D suspended gels, evidence of initial NMJ development was shown through colocalization of IF of cell-specific machinery and functional analysis of acetylcholine and glutamic acid stimulation. Video analysis showed calcium transients along uniaxially oriented myotube tracts after acetylcholine stimulation and using video analysis with ImageJ, we were able to measure myotube stimulation through calcium fluxes in myofibers in both mono- and coculture models. Limited evidence was also presented suggesting a differential response in myocytes after glutamate blockade following L-glutamic acid stimulation. L-Glutamic acid stimulation of myotubes theoretically occurs through activation of differentiated neurons, although analysis was difficult due to limited signal between glutamate activation above some spontaneous transients formed in the absence of simulation.

The development of force generating human myocytes *in vitro* has long been a goal of tissue engineering, although it has only been achieved in a small handful of laboratories dedicated to muscle differentiation research. Notably the first aneural spontaneous contraction in differentiated human myotubes was reported in 2014,[61] with the only 3D aligned *in vitro* human myotube contractions to date described by Madden *et al.* in 2015.[6] While myocyte activation was demonstrated with calcium transients in the present work, contractions that produced a measured force with reliability remained elusive and is an ongoing area of research.

Explanations for differences found between research groups using grossly similar protocols include batch variation in human cell isolates, as well as the intensive use of recombinant proteins and molecules in differentiation media in contraction producing variants. As this model thus far has not demonstrated force production of human muscle cells in culture it cannot yet detect any potential contraction force modulation with the addition of cocultured motoneurons. However, this model has demonstrated visualization of cytoarchitecture of both human motoneuron-like cells and differentiated myoblasts as well as the ability to measure signal transduction through both cell types, and will enable eventual force detection through measurement of cantilever force displacement.

This novel *in vitro* model of cocultured human myoblasts and motoneuron-like cells provides a customizable platform with potential for functional assaying of synaptic strength, plasticity, and contraction strength of muscle culture without limitation of encapsulating hydrogel used, assuming the availability of standard tissue cultureware and materials. Further development of this tissue model may serve as a potential alternative to costly animal studies and as a means for real-time analysis of patient-specific response to therapeutics. Currently, functional acetylcholine receptor clustering within engineering innervated skeletal muscle constructs allows for analysis of physiological neuron–muscle connectivity as well as a means to monitor the variety of pathological neuromuscular conditions in a controlled laboratory environment.

While the system in this work presents a novel functional toolkit and fills in a needed gap for neuromuscular analysis, models for the study of NMJs still have significant roadblocks before they are routinely sought after for translational and diagnostic purposes. This system does not currently have a precise method of integration of Schwann cells, which are known to be present in human NMJs. Precise segregation of neural cell bodies would also increase relevance to how motoneurons exist in the spinal cord. Further engineering methods, including optogenetics, may be added to this model, which will allow for stimulation of independent cell types in coculture, and may be used with more precise introduction of cell types with segregation of cell bodies to isolate specific cytoplasmic connections between cells present in the NMJ.

Conclusion

We have demonstrated primary human myoblasts reproducibly differentiated in 3D hydrogels in an anisotropic manner around freeform-printed polymerized silk fibroin cantilevers in standard tissue culture environments. Myoblasts can be differentiated in coculture with NG108-15 and hiNSC-derived motoneuron-like cells in 2D and 2.5D with mature cell-specific phenotypic expression, and lastly fully human 3D neuromuscular cocultures can be formed with active anisotropic myofiber function. This novel and scalable technique may be useful in future studies of disease models, and further studies will look at the potential for introducing more cell types, such as Schwann cells as well as optogenetic engineering of cell-specific stimulation.

Acknowledgments

The authors thank laboratory members Will Cantley, Will Collins, and Lorenzo Tozzi for discussion and technique, and Caroline McCormick for help with cell culture and bioprinting. They also thank the following Tufts faculty for additional mentorship and guidance: Li Zeng, Lauren Black, Jim Schwob, and Eric Frank. This study was funded by NIHP41 Tissue Engineering Resource Center Grant (EB002520) and R01 NS 092847.

Disclosure Statement

No competing financial interests exist.

References

1. Ijkema-Paassen, J., and Gramsbergen, A. Development of postural muscles and their innervation. Neural Plast **12,** 141, 2005.
2. Fidzianska, A. Human ontogenesis: II. Development of the human neuromuscular junction. J Neuropathol Exp Neurol **39,** 606, 1980.
3. Sanes, J.R., and Lichtman, J.W. Development of the vertebrate neuromuscular junction. Annu Rev Neurosci **22,** 389, 1999.
4. Liyanage, Y., Hoch, W., Beeson, D., and Vincent, A. The agrin/muscle-specific kinase pathway: new targets for autoimmune and genetic disorders at the neuromuscular junction. Muscle Nerve **25,** 4, 2002.
5. Murray, L.M., Talbot, K., and Gillingwater, T.H. Review: neuromuscular synaptic vulnerability in motor neurone disease: amyotrophic lateral sclerosis and spinal muscular atrophy. Neuropathol Appl Neurobiol **36,** 133, 2010.
6. Madden, L., Juhas, M., Kraus, W.E., Truskey, G.A., and Bursac, N. Bioengineered human myobundles mimic clinical responses of skeletal muscle to drugs. Elife **4,** e04885, 2015.
7. Murinson, B.B., Haughey, N.J., and Maragakis, N.J. Selected statins produce rapid spinal motor neuron loss in vitro. BMC Musculoskelet Disord **13,** 100, 2012.

8. Guo, X., Gonzalez, M., Stancescu, M., Vandenburgh, H.H., and Hickman, J.J. Neuromuscular junction formation between human stem cell-derived motoneurons and human skeletal muscle in a defined system. Biomaterials **32,** 9602, 2011.
9. Puttonen, K.A., Ruponen, M., Naumenko, N., Hovatta, O.H., Tavi, P., and Koistinaho, J. Generation of functional neuromuscular junctions from human pluripotent stem cell lines. Front Cell Neurosci **9,** 473, 2015.
10. Demestre, M., Orth, M., Föhr, K.J., *et al*. Formation and characterisation of neuromuscular junctions between hiPSC derived motoneurons and myotubes. Stem Cell Res **15,** 328, 2015.
11. Steinbeck, J.A., Jaiswal, M.K., Calder, E.L., *et al*. Functional connectivity under optogenetic control allows modeling of human neuromuscular disease. Cell Stem Cell **18,** 134, 2016.
12. Kalman, B., Monge, C., Bigot, A., Mouly, V., Picart, C., and Boudou, T. Engineering human 3D micromuscles with co-culture of fibroblasts and myoblasts. Comput Methods Biomech Biomed Engin **18(Suppl 1),** 1960, 2015.
13. Griffith, L.G., and Swartz, M.A. Capturing complex 3D tissue physiology in vitro. Nat Rev Mol Cell Biol **7,** 211, 2006.
14. Lund, A.W., Yener, B., Stegemann, J.P., and Plopper, G.E. The natural and engineered 3D microenvironment as a regulatory cue during stem cell fate determination. Tissue Eng B Rev **15,** 371, 2009.
15. Dhawan, V., Lytle, I., Dow, D., Huang, Y., and Brown, D.L. Neurotization improves contractile forces of tissue-engineered skeletal muscle. Tissue Eng **13,** 2813, 2007.
16. Wagner, S., Dorchies, O., Stoeckel, H., Warter, J., Poindron, P., and Takeda, K. Functional maturation of nicotinic acetylcholine receptors as an indicator of murine muscular differentiation in a new nerve-muscle co-culture system. Pflugers Arch **447,** 14, 2003.
17. Park, H.S., Liu, S., McDonald, J., Thakor, N., and Yang, I.H. Neuromuscular junction in a microfluidic device. Conf Proc IEEE Eng Med Biol Soc **2013,** 2833, 2013.
18. Morimoto, Y., Kato-Negishi, M., Onoe, H., and Takeuchi, S. Three-dimensional neuron-muscle constructs with neuromuscular junctions. Biomaterials **34,** 9413, 2013.
19. Larkin, L.M., Van Der Meulen, J.H., Dennis, R.G., and Kennedy, J.B.. Functional evaluation of nerve-skeletal muscle constructs engineered in vitro. In Vitro Cell Dev Biol Anim **42,** 75, 2006.
20. Gibbons, M.C., Foley, M.A., and Cardinal, K.O. Thinking inside the box: keeping tissue-engineered constructs in vitro for use as preclinical models. Tissue Eng Part B Rev **19,** 14, 2013.
21. Smith, A., Passey, S., and Greensmith, L. Characterization and optimization of a simple, repeatable system for the long term in vitro culture of aligned myotubes in 3D. J Cell Biochem **113,** 1044, 2012.
22. Smith, A.S.T., Long, C.J., McAleer, C., Bobbitt, N., Srinivasan, B., and Hickman, J.J. Utilization of microscale silicon cantilevers to assess cellular contractile function in vitro. J Vis Exp e51866, 2014.
23. Kim, M.S., Lee, B., Kim, H.N., *et al.* 3D tissue formation by stacking detachable cell sheets formed on nanofiber mesh. Biofabrication **9,** 015029, 2017.
24. Gholobova, D., Decroix, L., Van Muylder, V., *et al*. Endothelial network formation within human tissue-engineered skeletal muscle. Tissue Eng Part A **21,** 2548, 2015.
25. Merceron, T.K., Burt, M., Seol, Y.J., *et al.* A 3D bioprinted complex structure for engineering the muscle-tendon unit. Biofabrication **7,** 035003, 2015.
26. Choi, Y.-J., Kim, T.G., Jeong, J., *et al.* 3D cell printing of functional skeletal muscle constructs using skeletal muscle-derived bioink. Adv Healthc Mater **5,** 2636, 2016.
27. Smith, A.S.T., Long, C.J., Pirozzi, K., *et al*. A multiplexed chip-based assay system for investigating the functional development of human skeletal myotubes *in vitro*. J Biotechnol **185,** 15, 2014.
28. Smith, A.S.T., Long, C.J., Pirozzi, K., and Hickman, J.J. A functional system for high-content screening of neuromuscular junctions in vitro. Technology (Singap World Sci) **1,** 37, 2013.
29. Oleaga, C., Bernabini, C., Smith, A.S., *et al*. Multi-organ toxicity demonstration in a functional human in vitro system composed of four organs. Sci Rep **6,** 20030, 2016.
30. Regehr, K.J., Domenech, M., Koepsel, J.T., *et al*. Biological implications of polydimethylsiloxane-based microfluidic cell culture. Lab Chip **9,** 2132, 2009.
31. Rodriguez, M.J., Dixon, T.A., Cohen, E., Huang, W., Omenetto, F.G., and Kaplan, D.L. 3D freeform printing of silk fibroin. Acta Biomater **71,** 379, 2018.
32. Unger, R.E., Peters, K., Wolf, M., Motta, A., Migliaresi, C., and Kirkpatrick, C.J. Endothelialization of a non-woven silk fibroin net for use in tissue engineering: growth and gene regulation of human endothelial cells. Biomaterials **25,** 5137, 2004.
33. Wang, X., Kluge, J.A., Leisk, G.G., and Kaplan, D.L. Sonication-induced gelation of silk fibroin for cell encapsulation. Biomaterials **29,** 1054, 2008.
34. Włodarczyk-Biegun, M.K., and del Campo, A. 3D bioprinting of structural proteins. Biomaterials **134,** 180, 2017.
35. Das, S., Pati, F., Choi, Y.J., *et al*. Bioprintable, cell-laden silk fibroin–gelatin hydrogel supporting multilineage differentiation of stem cells for fabrication of three-dimensional tissue constructs. Acta Biomater **11,** 233, 2015.
36. Chaturvedi, V., Naskar, D., Kinnear, B.F., *et al*. Silk fibroin scaffolds with muscle-like elasticity support *in vitro* differentiation of human skeletal muscle cells. J Tissue Eng Regen Med **11,** 3178, 2017.
37. Yoshida, M., Kitaoka, S., Egawa, N., *et al*. Modeling the early phenotype at the neuromuscular junction of spinal muscular atrophy using patient-derived iPSCs. Stem Cell Rep **4,** 561, 2015.
38. Lee, P.H.U., and Vandenburgh, H.H. Skeletal muscle atrophy in bioengineered skeletal muscle: a new model system. Tissue Eng Part A **19,** 2147, 2013.
39. Aubin, H., Nichol, J.W., Hutson, C.B., *et al*. Directed 3D cell alignment and elongation in microengineered hydrogels. Biomaterials **31,** 6941, 2010.
40. Rockwood, D.N., Preda, R.C., Yücel, T., Wang, X., Lovett, M.L., and Kaplan, D.L. Materials fabrication from *Bombyx mori* silk fibroin. Nat Protoc **6,** 1612, 2011.
41. Cairns, D.M., Chwalek, K., Moore, Y.E., *et al*. Expandable and rapidly differentiating human induced neural stem cell lines for multiple tissue engineering applications. Stem Cell Rep **7,** 557, 2016.
42. Lu, Q., Hu, X., Wang, X., *et al*. Water-insoluble silk films with silk I structure. Acta Biomater **6,** 1380, 2010.
43. Carpenter, A.E., Jones, T.R., Lamprecht, M.R., *et al*. CellProfiler: image analysis software for identifying and quantifying cell phenotypes. Genome Biol **7,** R100, 2006.

44. Otsu, N. A threshold selection method from gray-level histograms. IEEE Trans Syst Man. Cybern **9,** 62, 1979.
45. Karl, D., Pavlin, M., and Sajn, L. Comparison of two automatic cell-counting solutions for fluorescent microscopic images. J Microsc **260,** 1, 2015.
46. Hinds, S., Bian, W., Dennis, R., and Bursac, N. The role of extracellular matrix composition in structure and function of bioengineered skeletal muscle. Biomaterials **32,** 3575, 2011.
47. Powell, C.A., Smiley, B.L., Mills, J., and Vandenburgh, H.H. Mechanical stimulation improves tissue-engineered human skeletal muscle. Am J Physiol Cell Physiol **283,** C1557, 2002.
48. Sato, M., Ito, A., Kawabe, Y., Nagamori, E., and Kamihira, M. Enhanced contractile force generation by artificial skeletal muscle tissues using IGF-I gene-engineered myoblast cells. J Biosci Bioeng **112,** 273, 2011.
49. Abbott, R.D., Kimmerling, E.P., Cairns, D.M., and Kaplan, D.L. Silk as a biomaterial to support long-term three-dimensional tissue cultures. ACS Appl Mater Interfaces **8,** 21861, 2016.
50. Yucel, T., Cebe, P., and Kaplan, D.L. Vortex-induced injectable silk fibroin hydrogels. Biophys J **97,** 2044, 2009.
51. Ko, I.K., Lee, B.K., Lee, S.J., Andersson, K.E., Atala, A., and Yoo, J.J. The effect of in vitro formation of acetylcholine receptor (AChR) clusters in engineered muscle fibers on subsequent innervation of constructs in vivo. Biomaterials **34,** 3246, 2013.
52. Choi, R.C., Yam, S.C., Hui, B., Wan, D.C., and Tsim, K.W. Over-expression of acetylcholinesterase stimulates the expression of agrin in NG108-15 cells. Neurosci Lett **248,** 17, 1998.
53. Lev, A., Feener, C., Kunkel, L., and Brown, R. Expression of the Duchenne's muscular dystrophy gene in cultured muscle cells. J Biol Chem **262,** 15817, 1987.
54. Shin, Y., Han, S., Jeon, J.S., *et al*. Microfluidic assay for simultaneous culture of multiple cell types on surfaces or within hydrogels. Nat Protoc **7,** 1247, 2012.
55. Shamir, E.R., and Ewald, A.J. Three-dimensional organotypic culture: experimental models of mammalian biology and disease. Nat Rev Mol Cell Biol **15,** 647, 2014.
56. Wu, W., and Manz, A. Rapid manufacture of modifiable 2.5-dimensional (2.5D) microstructures for capillary force-driven fluidic velocity control. RSC Adv **5,** 70737, 2015.
57. Uzel, S.G.M., Platt, R.J., Subramanian, V., *et al*. Microfluidic device for the formation of optically excitable, three-dimensional, compartmentalized motor units. Sci Adv **2,** e1501429, 2016.
58. Smith, A.S.T., Passey, S.L., Martin, N.R., *et al*. Creating interactions between tissue-engineered skeletal muscle and the peripheral nervous system. Cells Tissues Organs **202,** 143, 2016.
59. Scott, J.B., Ward, C.L., Corona, B.T., *et al*. Achieving acetylcholine receptor clustering in tissue-engineered skeletal muscle constructs in vitro through a materials-directed agrin delivery approach. Front Pharmacol **7,** 508, 2016.
60. Wang, L., Shansky, J., and Vandenburgh, H. Induced formation and maturation of acetylcholine receptor clusters in a defined 3D bio-artificial muscle. Mol Neurobiol **48,** 397, 2013.
61. Guo, X., Greene, K., Akanda, N., *et al*. In vitro differentiation of functional human skeletal myotubes in a defined system. Biomater Sci **2,** 131, 2014.

Address correspondence to:
David L. Kaplan, PhD
Department of Biomedical Engineering
Tufts University
4 Colby Street
Medford, MA 02155

E-mail: david.kaplan@tufts.edu

Received: February 19, 2018
Accepted: April 4, 2018
Online Publication Date: June 4, 2018